Lattice solution model for order-disorder transitions in membranes and Langmuir monolayers

Henrique S. Guidi[1,2,*] and Vera B. Henriques[1,†]

[1]*Instituto de Física, Universidade de São Paulo, P.O. Box 66318, 05314-970 São Paulo, SP, Brazil*

[2]*Centro de Ciências Físicas e Matemáticas, Universidade Federal de Santa Catarina, 88040-900 Florianópolis, SC, Brazil*

(Received 19 November 2013; revised manuscript received 13 July 2014; published 7 November 2014)

Lipid monolayers and bilayers have been used as experimental models for the investigation of membrane thermal transitions. The main transition takes place near ambient temperatures for several lipids and reflects the order-disorder transition of lipid hydrocarbonic chains, which is accompanied by a surface density gap. Equivalence between the transitions in the two systems has been argued by several authors. The two-state statistical model adopted by numerous authors for different properties of the membrane, such as permeability, diffusion, and mixture or insertion of cholesterol or protein, is inadequate for the description of charged membranes, since it lacks a proper description of surface density. We propose a lattice solution model which adds interactions with water molecules to lipid-lipid interactions and obtain its thermal properties under a mean-field approach. Density variations, although concomitant with chain order variations, are independent of the latter. The model presents both chain order and gas-liquid transitions, and extends the range of applicability of previous models, yielding Langmuir isotherms in the full range of pressures and areas.

DOI: 10.1103/PhysRevE.90.052705 PACS number(s): 87.16.D−, 68.47.Pe, 87.16.aj, 05.50.+q

I. INTRODUCTION

Lipid monolayers [1,2] and bilayers [3,4] have been extensively used as experimental models for the investigation of thermal and structural properties of the biological membrane. Phospholipid molecules form a monolayer film on the air-water interface, with lipid headgroups resting on water, while lipid hydrophobic chains acquire approximately parallel orientation in the air phase, thus avoiding contact with water. External lateral pressure guarantees aggregation into the monolayer film. Alternatively, in the water solution lipids aggregate into bilayer vesicles, as polar heads shield hydrocarbonic tails from contact with the aqueous medium. Bilayers are tension-free and aggregation is driven by the hydrophobic effect.

Both systems may undergo several phase transitions. The most thoroughly investigated of them is the pronounced order-disorder lipid chain transition, which displays latent heat, presented by either system. For lipid membranes temperature or *p*H variations may yield a so-called main gel-fluid transition. In the case of lipid monolayers, compression or heating disclose a transition traditionally known as a liquid-condensed liquid-expanded transition. The main transition involves two simultaneous phenomena: an abrupt variation in lipid surface density accompanied by disordering of the hydrocarbon chains. The latter acquire "kinks," while distance between polar headgroups increases, yielding decreased surface density. This is recognized as the chief effect also for bilayers [5–7], which undergo the main transition under temperature -variation.

There are different advantages in adopting either of the two experimental models. Direct measurement of surface area per lipid molecule, whose abrupt variation signals the transition, is possible only for monolayers. A lipid surface density gap develops for a range of applied external lateral pressures, at different temperatures. In the case of bilayers, a density gap arises at a single temperature, and the idea of application of lateral pressure lacks physical meaning. Bilayers are considered to be free of pressure. Nonetheless, equivalence between the two systems for a particular pressure on monolayers has been argued by many authors [8–10] and arguments rest on the assumption of negligible interaction between the two leaflets that compose the bilayer. Recent studies, however, indicate that this might be too strong a hypothesis [4]. Thus the question of equivalence is still controversial, and deserves further investigation.

Most of the well-established ideas on bilayer phase transitions refer to neutral lipid solutions. However, cell membrane lipids are often charged. Investigation of the behavior of charged lipid dispersions had a later start [11,12]. Charged lipid bilayers display a range of special properties. In particular, the main transition may develop into a broad transition, spanning several degrees of temperature, depending on chain length and ionic strength of the solution. The broad transition is accompanied by increased turbidity, viscosity, and conductivity [12]. Charge surface distribution undoubtedly plays a role [13,14], but interpretation of the thermal, electrical, viscous, and optical properties in terms of a molecular model is still lacking [11,12,15].

In this study, we investigate two features related to the molecular interpretation of chain order-disorder transition of lipid layers: (i) the statistical description of *surface density fluctuations*, which are essential in the analysis of charge surface density, as in the case of dissociating lipid, and (ii) the equivalence between monolayers and bilayers. Our approach is based on the proposal and investigation of a minimal statistical model which is a lattice solution version of a model introduced by Doniach [16] a few decades ago.

Computational facilities developed in the last decade or two allow the investigation of lipid layers through atomic detail model simulations [17–21] and also through mesoscopic models [22–26], which are nearer to a molecular description of the lipid systems, and yield a rich picture on the system macroscopic behavior. Nonetheless, the huge number of

*henrique@if.usp.br

†vera@if.usp.br

degrees of freedom of simulations for molecules with atomic detail, or even the reduced number of degrees of freedom, in the case of mesoscopic models, generally limit simulations to short times and to specific sets of model parameters. Alternatively, minimal models constitute an important instrument for probing ideas on the essential features behind macroscopic behavior, since results for any range of parameters, as well as the corresponding full phase diagrams, are achieved at very low computational cost. The latter features justify our focus on statistical models in the present study.

Different two-state and multistate models for lipid bilayers were proposed in the 1970s–1980s [16,27–29], inspired by the success of the two-state Ising model for magnetic systems [30]. The main ingredients considered by many authors were the different possible states for the lipid chains, associated with the ordered and disordered macroscopic phases, and the corresponding areas occupied by the lipid headgroups on the bilayer surface. A different approach rested on the analogy between the orientational order of lipid chains along the bilayer normal and the orientational order of nematic liquid crystals. Marcelja [7] proposed that chain kinks could be treated in terms of a nematiclike order parameter along the chain, subject to an effective field due to the density of extended chains. Area per lipid headgroup was taken as linearly dependent on the inverse of lipid chain length, from molecular volume conservation. On the other hand, the large enthalpy attributed to chain melting suggested that there could be an essentially entropic mechanism for the transition. Nagle [5] showed that an exact calculation of chain entropy could be achieved by complete enumeration of chain configurations through mapping on a dimer counting problem. However, the much simpler treatment of chain entropy in terms of an average degeneracy of the two-state model came to dominate the literature.

Caille and collaborators [27] considered a lattice of two-state lipid particles, corresponding to the two possibilities of ordered and disordered chains. Intramolecular chain entropy was attributed to a disordered lipid chain which would occupy a number of lattice sites. Doniach [16] simplified the two-state model of [27] by associating to each state a different area parameter, in an *ad hoc* fashion. This yielded the possibility of treating the resulting model exactly, through mapping on the seminal two-dimensional Ising model. Doniach's approach yielded the most successful statistical model for the main transition of neutral lipid layers. It serves as the basis for the study of different systems and properties involving neutral lipid systems: multicomponent lipid membranes, diffusive properties, or the effect of protein or cholesterol insertion [31–33].

Doniach's model describes the main transition in terms of the two states: an ordered extended chain and an average disordered chain. Surface area per lipid is taken as linearly dependent on the chain order parameter. The model is thus unable to describe local independent density fluctuations. This feature represents an important limitation of the two-state model, if one wishes to interpret the behavior of ionic lipid layers [12–15]. For dissociating lipids, electrostatic repulsion between lipid headgroups competes with attraction between lipid hydrocarbonic chains, due to the hydrophobic effect. Dissociation thus depends strongly on headgroup surface density, which must be described appropriately. A precise description of the local lipid surface density seems to be essential in order to rationalize thermal, electrical, and structural properties of the experimental system [15,34].

In this study, we consider a modified version of Doniach's model. Our purpose is twofold: (i) we introduce vacancies, in order to probe statistical surface density fluctuations, essential for the investigation of charged bilayers, and (ii) we insert water particles in the vacant sites, so that differences between monolayer and bilayer properties may be rationalized. We thus develop a lattice solution [35] version of Doniach's model, in which lattice sites may be occupied either by lipid or by water particles. The local surface density results from the equilibrium occupation of the lattice and the area per lipid is obtained from the statistics of the model. As a by-product of this approach, a "gas" phase is added to the original ordered and disordered "liquid" phases of Doniach's model. The new phases and new coexistence lines may be interpreted in terms of the transitions displayed by monolayers. Analysis of the behavior of the model system under pressure allows examination of the hypothesis of equivalence between monolayers and bilayers.

In Sec. II, we define the statistical model. In Sec. III, we present our mean-field approach. Results for the thermal behavior of density upon the order-disorder transition, as well as the model possible phase diagrams are displayed in Sec. IV. Physical interpretation in terms of the two systems of interest, monolayers and bilayers, is discussed in Sec. V. Final comments are given in Sec. VI.

II. DEFINITION OF THE STATISTICAL MODEL

We revise the seminal model proposed by Doniach a few decades ago [3,16,28] for the phospholipid bilayer main transition, in order to set notation. In Doniach's lattice model, lipid particles fill the plane lattice and are considered to visit two different particle states, an *ordered chain* state o [Fig. 1(a)], corresponding to an extended chain, and a highly degenerate *disordered chain* state d, meant to represent an average shortened chain [Fig. 1(b)]. Headgroup properties are assumed to play no role in relation to the bilayer transition.

The system consists of N particles distributed over the square lattice of $L^2 = N_o + N_d$ sites. Its configurational energy may be written as

$$E_{\text{Doniach}} = -\epsilon_{oo} N_{oo} - \epsilon_{dd} N_{dd} - \epsilon_{od} N_{od}, \tag{1}$$

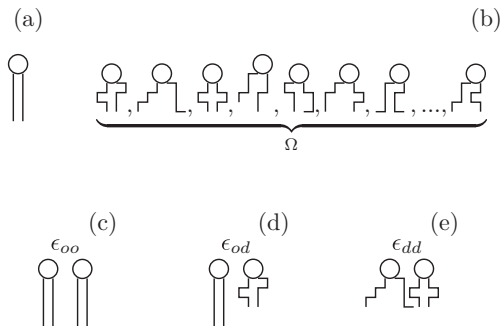

FIG. 1. (a) Simplified representation of a lipid with extended hydrocarbon chains. (b) Disordered chain configurations are represented through a single average disordered state of degeneracy Ω. (c)–(e) Interaction between pairs of lipids in different states.

where N_{xy} is the number of contacts between two particles in states x and y, and N_x is the number of lipids in state x, where $x = \{\mathrm{o,d}\}$ and $y = \{\mathrm{o,d}\}$. Interaction parameters ϵ_{xy} should all be taken as positive, since they represent effective attraction between particles. At the main transition, there is a sharp variation of the lipid chain states. A chain order parameter

$$m = \frac{N_\mathrm{o} - N_\mathrm{d}}{L^2} \tag{2}$$

describes chain order.

The model incorporates a second feature. Disordering of the chains is intimately related physically to loosening of the packing of lipid headgroups, as indicated by experiments. It seemed natural to make lipid area dependent on lipid chain state. Thus in Doniach's proposal a lipid particle in the ordered state could be associated with surface particle area a_o, while a lipid molecule in one of the disordered states would be given area a_d, with $a_\mathrm{d} > a_\mathrm{o}$. As a consequence, lattice and model areas have no correspondence, with $A \geqslant L^2 a_\mathrm{o}$, while $N_\mathrm{lip} = L^2$. This approach implies that the area per particle a_Doniach is defined as

$$a_\mathrm{Doniach} = \frac{N_\mathrm{o} a_\mathrm{o} + N_\mathrm{d} a_\mathrm{d}}{L^2}. \tag{3}$$

As can be seen, chain order parameter m and area per particle a_Doniach are not independent thermodynamic variables, since

$$a_\mathrm{Doniach}(m) = \tfrac{1}{2} m (a_\mathrm{o} - a_\mathrm{d}) + \tfrac{1}{2}(a_\mathrm{o} + a_\mathrm{d}). \tag{4}$$

The model simplicity allows mapping on a modified form of the two-state Ising magnetic model, whose thermodynamic properties are very well established [30]. Lateral pressure, conjugate to "area," acts as an effective field favoring the ordered phases. Together with temperature, this field controls the lipid system phases. Chains are ordered at large lateral pressures and low temperatures, as expected. At fixed temperatures, chains order discontinuously under increasing lateral pressure. As temperature increases, the transition disappears at a critical temperature.

Doniach's lattice solution model—DLG

As announced previously, we introduce vacancies which are filled with water particles, and write Doniach's model as a lattice solution with explicit water particles.

Lipids are amphiphilic molecules constituted of hydrophobic hydrocarbonic chains and hydrophilic polar heads. Thus lipid chains avoid contact with water by turning to the air phase in the case of monolayers, while in the case of bilayers they turn towards the bilayer core.

In our model, interaction between lipid and water particles is described through a "van der Waals"-like short-range potential $\epsilon_\mathrm{w,lip}$, while water particles interact via a first-neighbor interaction ϵ_ww, with $\epsilon_\mathrm{ww} > \epsilon_\mathrm{w,lip}$, in order to represent the strong preference for water particles to bond between themselves, which is the basis of the hydrophobic effect.

In this proposal, the fixed relation between area per particle, a, and chain parameter m, Eq. (4), is abandoned, since in the new model chain order parameter and lipid density vary independently. Figure 2 illustrates pictorially our proposal, as compared to the original Doniach description.

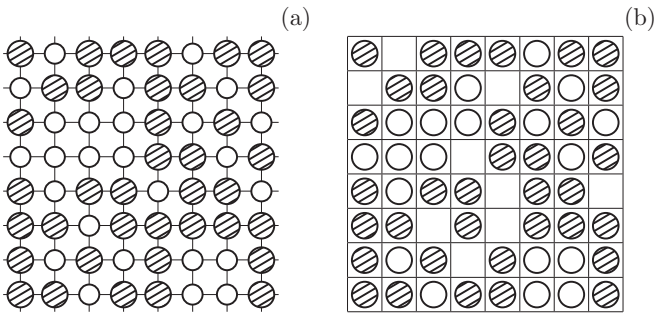

FIG. 2. (a) Illustration of Doniach's model. Lipid states define area per lipid, which is independent of lattice spacings. (b) A lattice gas version of Doniach's model (DLG). Sites are occupied either by lipid or water particles. Area per lipid is obtained from model statistics.

Let us consider a square lattice which may be occupied by lipids or by water. The lipid particle chains may be either in the ordered or disordered state. Interactions between lipid particles are the same as those of Eq. (1), to which lipid-water and water-water interactions are added. Model energy reads

$$\begin{aligned} E &= E_\mathrm{Doniach} + E_\mathrm{lip\text{-}water} \\ &= -\epsilon_\mathrm{oo} N_\mathrm{oo} - \epsilon_\mathrm{od} N_\mathrm{od} - \epsilon_\mathrm{dd} N_\mathrm{dd} \\ &\quad - \epsilon_\mathrm{ow} N_\mathrm{ow} - \epsilon_\mathrm{dw} N_\mathrm{dw} - \epsilon_\mathrm{ww} N_\mathrm{ww}, \end{aligned} \tag{5}$$

where indices $x, y = \mathrm{o,d,w}$ are associated with lipids in the ordered state o, lipids in disordered state d, and water particles w. Accordingly, N_{xy} is the number of contacts between sites occupied by lipids o, by lipids d, or by water particles w. As in Doniach's model, the disordered states are multiply degenerate, the degeneracy Ω corresponding to the high entropy of the disordered hydrocarbon chains of a single lipid. Note that the number of lipid particles $N_\mathrm{lip} = N_\mathrm{o} + N_\mathrm{d}$ is *not* fixed, $N_\mathrm{lip} \neq L^2$.

In order to give our model a statistical treatment, it is convenient to rewrite energy [Eq. (5)] in terms of statistical variables. A direct representation of Eq. (5) would be

$$E = \sum_x \sum_y -\epsilon_{xy} \sum_{(ij)} \eta_i^x \eta_j^y, \tag{6}$$

where $\eta_i^x = 1$, if site i is occupied by particle x, or $\eta_i^x = 0$, if site i is occupied by particle $y \neq x$. $\sum_{(ij)}$ is the sum over pairs of nearest neighbors i and j.

A simpler expression of energy [Eq. (5)] in terms of mathematical manipulations may be written, if we attribute variables σ to lattice sites as in Table I. Under this representation, we obtain

$$\begin{aligned} E &= E_\mathrm{int} + E_\mathrm{hydr} + E_0 \\ &= -J \sum_{(ij)} \sigma_i \sigma_j - \Delta \sum_{(ij)} \sigma_i \sigma_j (\sigma_i + \sigma_j) \\ &\quad - K \sum_{(ij)} \sigma_i^2 \sigma_j^2 + I \sum_i \sigma_i^2 - 2\epsilon_\mathrm{ww} L^2, \end{aligned} \tag{7}$$

TABLE I. Particle states and statistical variables.

Particle	Occupation variable σ	Mapping $\sigma \to \eta$ $\eta^x(\sigma)$
Ordered chain lipid (o)	1	$\eta^{\mathrm{o}} = \frac{1}{2}\sigma^2(1+\sigma)$
Disordered chain lipid (d)	–1	$\eta^{\mathrm{d}} = \frac{1}{2}\sigma^2(1-\sigma)$
Water (w)	0	$\eta^{\mathrm{o}} = 1-\sigma^2$

where, for simplicity, new interaction parameters are defined as

$$J = \frac{\epsilon_{\mathrm{oo}} + \epsilon_{\mathrm{dd}} - 2\epsilon_{\mathrm{od}}}{4}, \tag{8}$$

$$\Delta = \frac{\epsilon_{\mathrm{oo}} - \epsilon_{\mathrm{dd}} - 2\epsilon_{\mathrm{ow}} + 2\epsilon_{\mathrm{dw}}}{4}, \tag{9}$$

$$K = \frac{\epsilon_{\mathrm{oo}} + \epsilon_{\mathrm{dd}} + 2\epsilon_{\mathrm{od}} + 4\epsilon_{\mathrm{ww}} - 4\epsilon_{\mathrm{ow}} - 4\epsilon_{\mathrm{dw}}}{4}, \tag{10}$$

and

$$I = 2(2\epsilon_{\mathrm{ww}} - \epsilon_{\mathrm{ow}} - \epsilon_{\mathrm{dw}}). \tag{11}$$

Note that the first three terms constitute lipid-lipid interaction terms, represented as E_{int}, the fourth term represents a hydrophobic "field" term E_{hydr}, while the last term is a constant E_0.

The only term present in Doniach's model is the first term, which means that entirely new behavior might emerge from the added degrees of freedom. The two new lipid interaction terms, of coefficients Δ and K, arise as a result of the introduction of vacancies. $J > 0$ governs the lipid-lipid interactions, and favors lipid neighboring pairs in the same state. $\Delta > 0$ governs the stability of the ordered state. $K > 0$ favors both site occupation by lipids and lipid-lipid contacts, independently of lipid state. The introduction of water particles yields the "field" term, and $I > 0$ favors water occupation of sites.

In the case of our model, equilibrium properties are more easily calculated in the grand-canonical ensemble. The grand-partition function reads

$$\Xi(T, \mu_{\mathrm{lip}}, \mu_{\mathrm{w}}) = \sum_{\{\sigma\}} \Omega^{N_{\mathrm{d}}} e^{-\beta\left(E - \mu_{\mathrm{lip}} N_{\mathrm{lip}} - \mu_{\mathrm{w}} N_{\mathrm{w}}\right)}, \tag{12}$$

where μ_{lip} and μ_{w} are the lipid and water chemical potentials, respectively, and $\beta = \frac{1}{kT}$. The total number of lipid particles N_{lip}, the number of water particles N_{w}, and the number of disordered chain lipids N_{d} are given respectively by

$$N_{\mathrm{lip}} = \sum_i \sigma_i^2, \tag{13}$$

$$N_{\mathrm{w}} = L^2 - N_{\mathrm{lip}}, \tag{14}$$

and

$$N_d = \sum_i \sigma_i^2(1-\sigma_i)/2. \tag{15}$$

It is interesting, at this point, to note that the linear "hydrophobic" energy term in the energy expression [Eq. (7)] competes with the chemical potential factor, so we rewrite the grand-partition function as

$$\Xi(T,\mu) = e^{\beta(\mu_{\mathrm{w}} + 2\epsilon_{\mathrm{ww}})L^2} \sum_{\{\sigma\}} \Omega^{N_{\mathrm{d}}}(\sigma) e^{-\beta[E_{\mathrm{int}}(\{\sigma\}) - \mu N_{\mathrm{lip}}(\{\sigma\})]}, \tag{16}$$

where we define an "effective" chemical potential μ, given by

$$\mu \equiv \mu_{\mathrm{lip}} - \mu_{\mathrm{w}} - I. \tag{17}$$

III. MEAN-FIELD APPROACH

The model equilibrium properties may be obtained from a Curie-Weiss mean-field approach [36], which yields analytical expressions for the system's equations of state. Under this approach, interactions are made independent of distance, with the replacement

$$\sum_{(i,j)} X_i X_j \to \frac{2}{A} \sum_i X_i \sum_j X_j, \tag{18}$$

for the square lattice, where X_i are interaction variables. The model energy interaction term is written as

$$E_{\mathrm{int,\,MF}} = \frac{2}{L^2}\left(-JM^2 - 2\Delta M N_{\mathrm{lip}} - K N_{\mathrm{lip}}^2\right), \tag{19}$$

where N_{lip}, defined by Eq. (13), is the number of lipid particles for a given microstate, and M is defined as

$$M = \sum_i \sigma_i. \tag{20}$$

The mean-field energy interaction term, Eq. (19), replaces the original interaction term [see Eq. (7)] in the Boltzmann factor of the grand-partition function, Eq. (16). Then, linearization of quadratic terms in M and N_{lip} which appear in the Boltzmann weights may be achieved through two Gaussian transformations such as

$$e^{y_{1,2}^2} = \frac{1}{\sqrt{\pi}} \int_{-\infty}^{\infty} e^{-x_{1,2}^2 + 2y_{1,2}x_{1,2}} dx. \tag{21}$$

Summation over statistical variables σ becomes straightforward. After summation, integrals in variables x introduced by the Gaussian transformations must be solved by the steepest descent method. For large systems the main contribution comes from extrema of the exponential factor which yield the system's grand potential. We obtain the following grand potential $\Phi(T, A, \mu, H)$:

$$\frac{\Phi(T,A,\mu,H;m,n)}{L^2} = 2(Jm^2 + Kn^2 + 2\Delta nm) - 2\epsilon_{\mathrm{ww}} - \mu_w - \frac{1}{\beta}\ln(1+\phi_+). \tag{22}$$

The functions ϕ_+ are defined as

$$\begin{bmatrix}\phi_+ \\ \phi_-\end{bmatrix} = e^{\beta(4\Delta m + 4Kn + \mu - \frac{1}{2}I)} \times \left(e^{\beta(4Jm + 4\Delta n)} \begin{bmatrix}+\\-\end{bmatrix} \Omega e^{-\beta(4Jm+4\Delta n)}\right). \tag{23}$$

m and n correspond to the integration variables x_i, $i = 1,2$ at the conditions for the extrema of the arguments of the

exponentials in the Gaussian integrals [Eq. (21)], and are given by the set of coupled equations

$$\begin{bmatrix} m \\ n \end{bmatrix}(T,\mu;m,n) = \begin{bmatrix} \phi_- \\ \phi_+ \end{bmatrix} \frac{1}{1+\phi_+}. \tag{24}$$

From thermodynamics, m and n are identified, respectively, as the chain order parameter m, given by

$$m = \frac{\langle M \rangle}{L^2} = \frac{N_o - N_d}{L^2} = \frac{N_{lip} - 2N_d}{L^2} \tag{25}$$

from Eqs. (2), (13), and (15), and the lipid surface density n, defined as $n = \langle N_{lip} \rangle / L^2$ [see Eq. (13)].

Equation (24) may be solved numerically for any set of model parameters. Possible solutions and the associated lipid system phases are presented and discussed in the following section.

IV. SURFACE DENSITY AND PHASE DIAGRAM

Model properties are investigated through inspection of the solutions for chain order parameter $m(T,\mu)$ and lipid density $n(T,\mu)$ [Eqs. (23) and (24)]. Given the stable solutions, we construct the overall phase diagrams.

For simplicity, all our results are given in terms of dimensionless variables and parameters, defined below:

$$t = k_B T/J, \tag{26}$$

$$\overline{\mu} = \frac{\mu}{J}, \tag{27}$$

$$\overline{K} = \frac{K}{J}, \tag{28}$$

and

$$\overline{\Delta} = \frac{\Delta}{J}, \tag{29}$$

with J, K, Δ, and μ given by Eqs. (8), (9), (10) and (17), respectively.

Depending on the thermodynamic parameters, $\overline{\mu}$ and t, several solutions may be found for $m(T,\mu)$ and $n(T,\mu)$ [Eqs. (23) and (24)], and the equilibrium physical solution is obtained from inspection of the global minimum of the grand-potential Φ [Eq. (23)]. Figures 3(a)–3(d) illustrate this procedure. m and n present different numbers of solutions under temperature variation at fixed chemical potential, as can be seen, respectively, in Figs. 3(a) and 3(b). Dashed lines represent unstable solutions; solid lines represent the solutions of minimum thermodynamic potential [see Fig. 3(d)]. Note that the disordering transition of the chains, signaled by the abrupt discontinuity in chain parameter m, is accompanied by a small discontinuous transition in density n, shown in detail in Fig. 3(c). We shall return to this point later.

A possible overall phase diagram is displayed in Fig. 4, for a specific set of parameters. Three phases are present: a gas phase (Gas), characterized by very low density ($n \approx 0$); a liquid of ordered chains (Ord), of density $n \approx 1$, with chain parameter $m \approx 1$; and a liquid of disordered chains (Dis), of density $n \approx 1$, with chain parameter $m \approx -1$. The gas phase is present at low chemical potentials. At low fixed temperature, a Gas-Ord transition takes place as chemical potential is increased. For higher chemical potentials, as one increases temperature, a discontinuous Ord-Dis transition occurs, with a small density gap in density n accompanying a sharp transition in chain order parameter m, from 1 to -1. For a range of intermediate chemical potentials, raising temperature produces a Gas-Dis discontinuous transition in density n, which ends at at a critical point. The three phases coexist at a triple point.

Reentrant behavior is displayed near the triple point, as one raises temperature, in a small range of fixed chemical potentials μ. This is shown in the inset of Fig 4: As the temperature is increased, the ordered chains give rise to a gas phase, and as temperature is increased further, the gas phase presents coexistence with a disordered chains liquid.

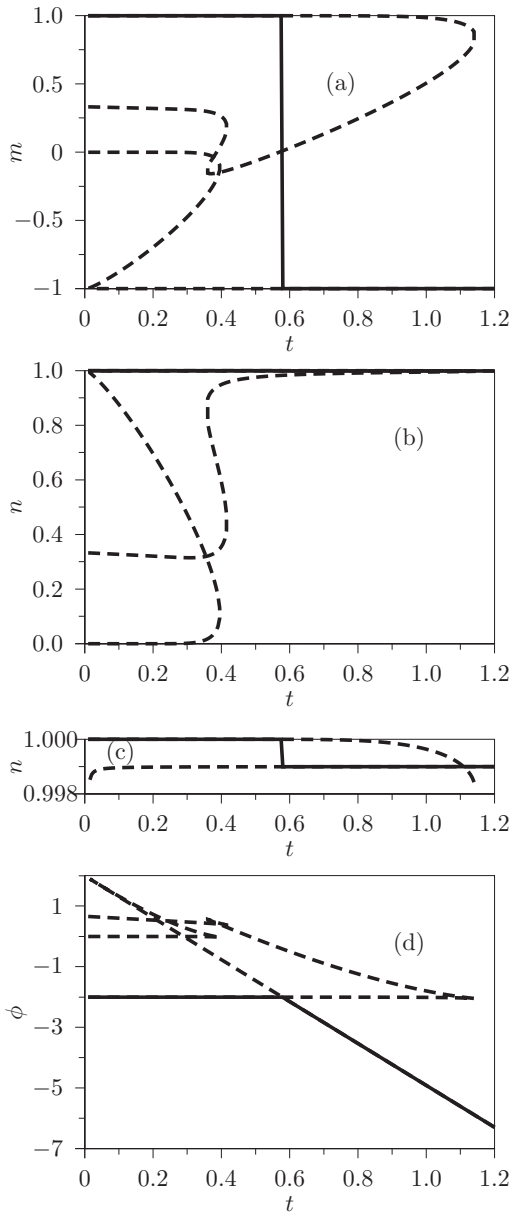

FIG. 3. Chain order parameter m (a), lipid surface density n (b), from Eq. (24), and thermodynamic potential Ψ (d), from Eq. (23) vs reduced temperature t. A detail of the discontinuity in density is displayed in (c). Continuous lines indicate stable solutions. $\overline{\Delta} = 0.5$, $\overline{K} = 1$, $\overline{\mu} = -4$, and $\Omega = 1000$.

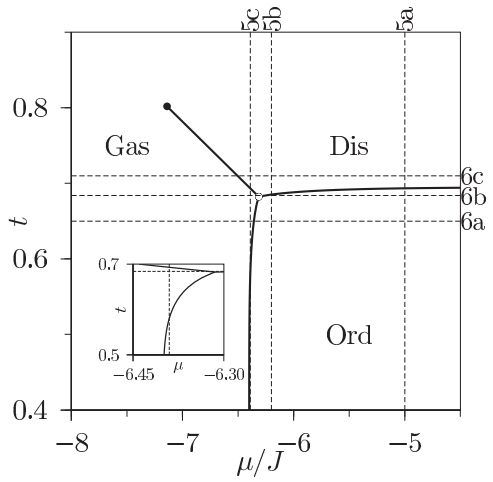

FIG. 4. Temperature t vs chemical potential $\overline{\mu}$ phase diagram. Continuous lines are coexistence lines. The open circle indicates the triple point and the solid circle indicates the critical point. m and n behavior along the dashed lines are illustrated in Figs. 5 and 6. $\overline{\Delta} = 0.6$, $\overline{K} = 1$, and $\Omega = 1000$.

The different phases across the phase diagram are illustrated in Figs. 5 and 6, in terms of the behaviors of surface density $n(T,\mu)$ and chain order parameter $m(T,\mu)$.

Figure 5 displays the behavior patterns for m and n under temperature variations, at different fixed chemical potentials. At higher μ, the Ord-Dis chain transition, with m going from $+1$ to -1, is accompanied by a density gap in n, which yields a discontinuity in the area per lipid at the transition. Nearer to the triple point, discontinuity in density at the Ord-Dis transition increases [compare Figs. 5(d) and 5(e)]. Reentrant behavior takes place beyond the triple point, Figs. 5(c) and 5(f), with an Ord-Gas transition following a Gas-Dis transition, as temperature is raised. The different phase transitions of Fig. 5 develop along the vertical dashed lines in the phase diagram of Fig. 4.

Figures 6(a)–6(f) display the behavior of chain parameter m and lipid density n as the chemical potential is raised, at fixed temperature. The Gas-Ord transition at low temperatures, below the triple point, is signaled by a discontinuity in m from 0 to 1, with a density jump from ≈ 0.1 to 1 [Figs. 6(a) and 6(d)]. At the intermediate temperature, just below the triple point, the Gas-Dis transition is followed by a Dis-Ord transition, with two discontinuities in density [Figs. 6(b) and 6(d)]. Finally, at higher temperature, above the triple point, a Gas-Dis transition is accompanied by a density jump between densities 0.2 and 0.8 [Figs. 6(c) and 6(e)]. The horizontal dashed lines of Fig. 4 indicate the different phase transitions of Fig. 6.

At this point, it is interesting to underline one of the results we sought: a description of surface density n independent of the chain order parameter m. In the original model by Doniach for lipid bilayers, the two parameters were linearly coupled through Eq. (4). An inspection of Figs. 3(c), 5(b), and 5(e) shows that in our DLG model n and m are decoupled, since $\Delta n \approx 0.001$, $\Delta n \approx 0.01$, and $\Delta n \approx 0.1$, respectively, whereas $\Delta m \approx 2$. As for Doniach's model, the latter value for Δm would yield $\Delta n \approx 0.3$, for all three cases, if a reasonable value for a_d/a_o, around 1.2 is adopted [15].

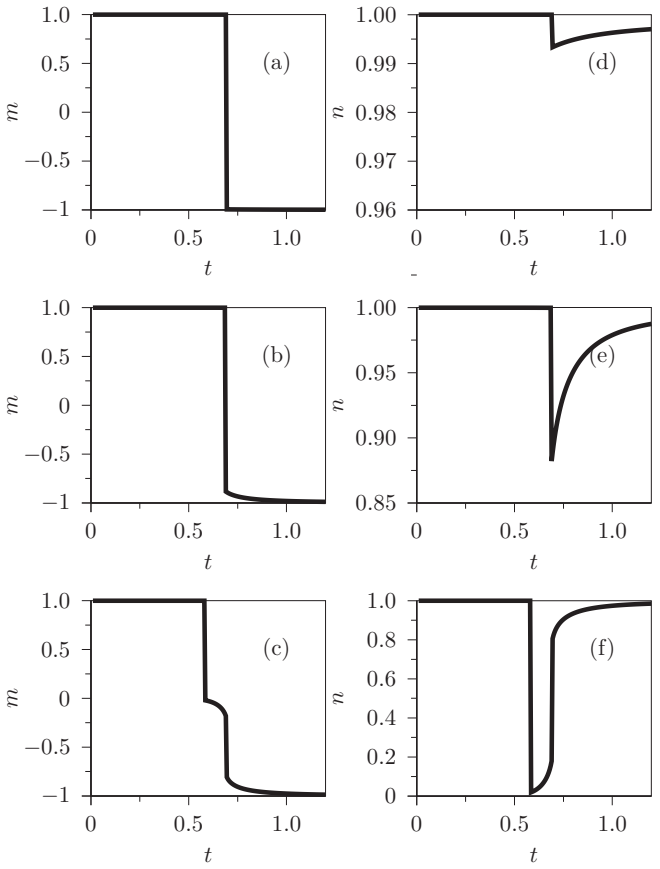

FIG. 5. Chain order parameter m [(a)–(c)] and lipid surface density n [(d) and (e)] vs t, for fixed $\overline{\mu} = -5$, -6.2, and -6.39, shown as dashed vertical lines in the phase diagram of Fig. 4.

What is the effect of varying model parameters upon the phase diagram? Figure 7(a) illustrates the effect of variation of parameter Δ at fixed K, while Fig. 7(b) illustrates the effect of varying K at fixed Δ.

In Fig. 7(a) we see that the gas-order line moves to higher chemical potentials and the critical point disappears as K is lowered. Figure 7(b) shows that increasing Δ dislocates both the gas-ordered chains coexistence line as well as the order-disorder line, while the critical point disappears.

An inspection of the role of the interaction parameters in the expression for energy [Eq. (7)] explains some of the features displayed by the different phase diagrams. Parameter K favors states $\sigma = +1$ and $\sigma = -1$ and thus the filling of the lattice by lipids, at low temperatures. This explains why the gas-ordered liquid transition, at low temperatures, is moved towards a lower chemical potential μ, as K is increased. On the other hand, parameter Δ favors particle state $\sigma = +1$, and thus stabilizes the ordered chains liquid state, moving the low temperature gas-liquid transition to lower chemical potential μ and the ordered chain liquid–disordered chain liquid transition to higher temperature T. Dislocation of the coexistence lines might yield the disappearance of the Gas-Dis line, and therefore of the triple and critical points. This is the case both for $K = 0.8$ ($\Delta = 0.6$) in Fig. 7(a) and for $\Delta = 0.7$ ($K = 1$) in Fig. 7(b).

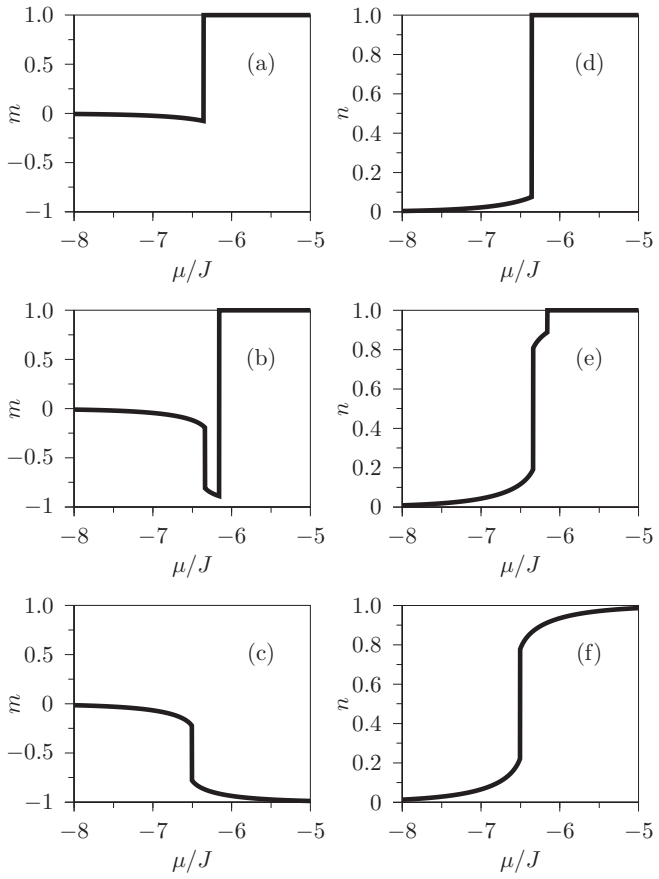

FIG. 6. (a) Isothermal m and n transitions $vs\overline{\mu}$ for $t = 0.65$ [(a) and (d)], 0.684 [(b) and (e)], and 0.71 [(c) and (f)]. The three temperatures are indicated as dashed lines in the phase diagram of Fig. 4.

Note that the two coexistence lines, gas liquid and ordered-disordered liquid may either merge continuously or meet at a triple point. But why does the coexistence line between the gas and the disordered chain liquid disappear, as Δ is increased at fixed K or as K is lowered at fixed Δ? In fact, the presence of the three phases and of the transitions between them may be rationalized from analysis of the three limiting models which are combined in the Doniach lattice solution we propose: a lattice-gas model, a degenerate lattice-gas model, and Doniach's model. Analysis of the phase diagrams of Fig. 7 in terms of the limiting models is given in the Appendix.

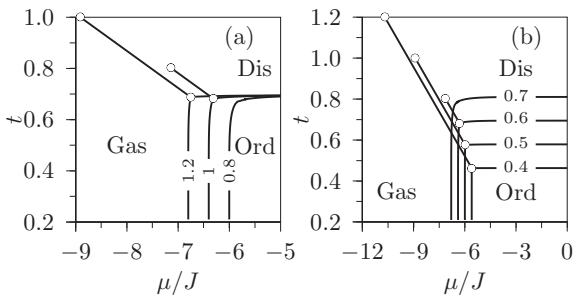

FIG. 7. Model phase diagrams depend on model parameters. In (a), $\overline{\Delta} = 0.6$, with $\overline{K} = 0.8, 1, 1.2$. In (b), $\overline{K} = 1$, with $\overline{\Delta} = 0.4$–0.7.

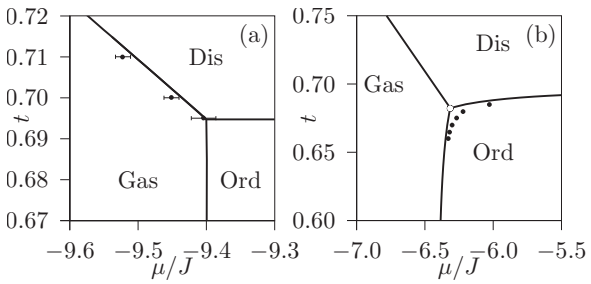

FIG. 8. Monte Carlo vs mean-field phase diagram for $\overline{\Delta} = 0.6$. Continuous lines correspond to mean-field results and points are results of simulations: (a) $\overline{K} = 2.5$; (b) $\overline{K} = 1.0$, $\Omega = 1000, L = 32$ in MC simulations. Error bars in (b) are the size of the symbols.

In order to check the mean-field (MF) analysis, which might, in some cases, even yield wrong predictions with respect to the presence of criticality [37,38], which might be relevant for the lipid order-disorder transition [39], we have done some exploratory Monte Carlo (MC) simulations [40]. In Fig. 8 we compare mean-field and Monte Carlo results for the model phase diagram for the two sets of interaction parameters. The differences to be noted are (i) the Gas-Dis line is present for both values of K in the mean-field approach, whereas in the case of Monte Carlo results this line is present only for the larger value of K; (ii) Monte Carlo and mean-field results for the two other coexistence lines coincide except in the region of the triple point. Both features are easily explained: Because the mean-field approach does not take into account correlations it always yields higher critical temperatures than exact calculations [30]. Thus, the critical temperature at the end of the Gas-Dis line is significantly smaller in the case of Monte Carlo simulations, as compared with the case of mean-field calculations. The critical point may even become unstable, falling inside the Ord phase, with effects on the nearby coexistence lines, as is the case in Fig. 8(b). Note in Fig. 7(a) that the MF critical temperature of the Gas-Dis line goes up as K is increased at fixed Δ, but collapses onto the order-gas line at small K. Thus, for $\overline{\Delta} = 0.6$, the MF approach predicts a critical point for $\overline{K} > 0.8$, while in the MC approach this critical point appears only for $\overline{K} > 1.4$ (see Appendix for details). In conclusion, MC results confirm our predictions for the model phase diagram, with divergent numerical results only near the critical point, which is not itself the focus of our study.

Finally, in order to be able to discuss relevance with respect to the experimental systems, we obtain the model pressure-temperature phase diagram. From thermodynamics, lateral pressure $p_{\rm lat}$, conjugate to area A, is given by

$$p_{\rm lat} = -\frac{1}{A}\Phi(T, A, \mu, H). \tag{30}$$

For our model, the thermodynamic grand potential Φ is given by Eq. (23).

Figure 9 displays the lateral pressure $p_{\rm lat}$ versus temperature t phase diagram, for the same model parameters as in Fig. 4, in terms of reduced pressure, defined by

$$\Pi = \frac{a_{\rm ord}\, p_{\rm lat}}{J}. \tag{31}$$

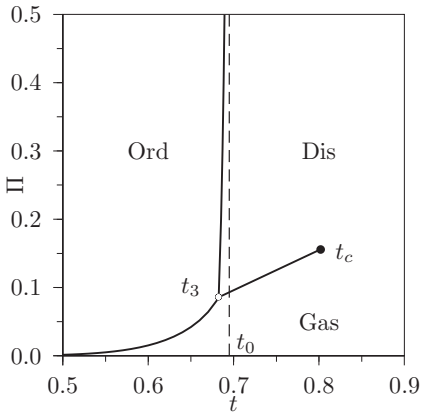

FIG. 9. Reduced lateral pressure Π vs temperature t. t_3 and t_c indicate the temperatures of the triple and critical points, respectively (see Fig 4). The dashed line indicates the high density limit of the order-disorder transition, temperature t_0. Parameters are the same as Fig 4.

The gas phase is present at low pressure and higher temperatures, as for usual fluids. At higher pressures, the two fluid phases are separated by a coexistence line, Π with the liquid of ordered chains (Ord) at lower temperatures, and the liquid of disordered chains (Dis) at higher temperatures. The coexistence pressure $\Pi_{\text{ord-dis}}$ between the two liquid phases rises steeply as temperature is increased. The asymptotic value of the corresponding transition temperature, $t_{\text{ord-dis}}$, is indicated as t_0. At low pressure, chain disordering is accompanied by a density gap, which goes exponentially to zero as pressure is increased.

Interpretation of the Π vs t phase diagram in terms of physical parameters for the lipid systems is discussed in the following section.

V. PHYSICAL INTERPRETATION: MONOLAYERS VS BILAYERS

In order to interpret our findings in terms of the two systems of interest, monolayers and bilayers, we must analyze the differences between *interparticle interactions* in the two systems, as well as the difference between the *physical boundary conditions* involved.

The anisotropic organization of the phospholipid molecules in layers is a consequence of the fact that those are amphiphilic molecules, with a hydrophylic polar headgroup which mixes with water and a hydrophobic hydrocarbonic tail which would phase separate were it not attached to the polar headgroup. The nematiclike structure, in which chains order perpendicularly to the layer surface, is common to bilayers and monolayers. However, there are specific aspects of the *interactions* between lipids and water which make them different physical systems. While lipid headgroups are in contact with water in both systems, the same is not true for hydrocarbonic tails. In the case of monolayers, the hydrophobic lipid chains turn to the air subphase and have no contact with water, independently of the distance between lipids. As to bilayers, hydrophobic chains turn to the hydrophobic bilayer core, but water penetration increases as lipid molecules move apart. Thus, if the average bilayer surface density decreases, lipid tails get in contact with water, which does not occur with lipids in the monolayer. A relevant consequence of these facts, in relation to comparison to experiments, is that interaction constants $\epsilon_{\text{lip,w}}$ of the model we propose will not be the same for both systems.

A second feature which must be distinguished between the two experimental systems is the range of thermodynamic space available for each system. Monolayers may be manipulated both through direct compression, as well as through heating, implying a line of disordering transitions in the pressure-temperature plane. Bilayer behavior is probed through temperature variations only, and the disordering transition occurs at a single temperature and "internal pressure."

In the following sections we analyze the differences pointed out above and the relation between the two physical systems and our model.

A. Monolayers

A monolayer is constituted of lipid particles, whose chains suffer van der Waals attraction. Lipid headgroups rest on the water surface, and lipid chains do not get in contact with water molecules, which allows us to take lipid-water interactions independent of the lipid chain state, $\epsilon_{\text{lip,w}} = \epsilon_{\text{ow}} = \epsilon_{\text{dw}}$. On the other hand, water-water "bonds" are surface bonds, from now on labeled as $\epsilon_{\text{ww}}^{\text{surf}}$. When lipid molecules become dispersed, water molecules attract strongly between themselves yielding large surface tension. At very low temperature and very low pressure, one expects the model system to go into a "gas" lipid phase, since water-water interactions are dominant over lipid-lipid interactions.

Much of the experimental investigation of monolayers is given in terms of Langmuir pressure-area isotherms, which present two coexistence plateaus, one between the gas and the expanded liquid, at lower pressure, and the second one between the expanded and the condensed liquid phases [1,2], for which the discontinuity in area per molecule is an order of magnitude lower. If compression is further increased, collapse of the monolayer comes about [41].

Our model pressure-temperature isotherms are displayed in Fig. 10. It can be seen that they compare well qualitatively to experimental plots [42]. Both transitions are present, at different orders of magnitude, both for pressure and area per molecule. Isotherm temperatures are referred to the high density limit of the order-disorder transition, t_0 (see Fig. 9), and are given as $(t - t_0) \times 1000$. Inspection of Fig. 9 shows that two plateaus on the same isotherm should be expected only in the interval $t_3 < t < t_0$. The order-disorder plateau [Fig. 10(a)] is present for $t_3 < t < t_0$ and the area gap is limited to $\approx 20\%$ upon the transition. The gas-liquid plateau [Fig. 10(b)] remains present beyond the asymptotic temperature t_0 up to the critical temperature t_c, at much smaller pressures. In the latter case, pressures are an order of magnitude lower, and area may vary by a factor of 10. The lattice, of course, limits the minimum area, so that isotherms increase steeply at the lower limit, differently from the experimental system, which, besides, may expand into a third dimension [41].

A critical point for the Ord-Dis transition is absent for the parameters explored in this study. However, it may be present for a different set of parameters, as explained in the Appendix.

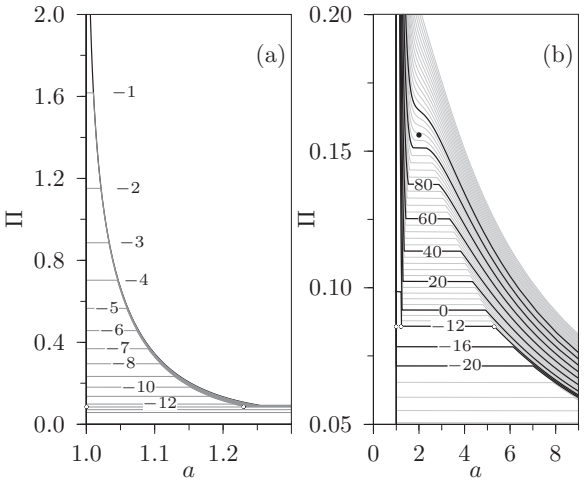

FIG. 10. Pressure vs lipid area isotherms. Temperatures are given in terms of the relative temperature $(t - t_0) \times 1000$ (see Fig. 9). (a) Isotherms present a plateau associated with the order-disorder transition for $t_3 < t < t_0$. (b) Isotherms present a plateau associated with the gas-(disordered)liquid transition for $t_3 < t < t_0$. See text for details. Model parameters are as in Fig. 4.

B. Bilayers

In the case of a bilayer, the gas-liquid transition would correspond to membrane disaggregation and some critical micellar (or vesicular) parameter [43], which is not of interest in the study of biomembranes. Thus the Gas-Dis line of Fig. 9 may be considered of no relevance in the case of bilayers.

As for the integral vesicle thermal phases, water-water and water-lipid interactions are essential. Water-water bonds in the bulk are "looser" than at the surface, and we thus label them as ϵ_{ww}^{bulk}. More importantly, the competition between both intermolecular interaction constants is the source of the "hydrophobic" interaction, $\epsilon_{hydroph} \equiv \epsilon_{ww}^{bulk} - \epsilon_{lip,w}$. The latter is considered to guarantee the stability of the vesicle aggregate, which, differently from monolayers, lacks the need for an external "aggregating force." Thus, bilayers are considered to be in a tension-free state, which would correspond [9,10,44] to a situation of zero lateral pressure Π. Yet, different authors propose an equivalence between the pressure-free bilayer and the monolayer at some specific lateral pressure [9,10]. The equivalence between the two systems would allow utilization, for bilayers, of data from the experimental investigation of monolayers. Under the equivalence hypothesis, bilayers should be represented by a single horizontal line above the triple point, in the pressure-temperature phase diagram of Fig. 9.

In the next section, we discuss a possible rationalization of the restrictions to the proposed equivalence, which have been suggested to exist [44], since one is unable to obtain simultaneous correspondence of the transition temperature and of the area gap, at the same lateral pressure.

C. Bilayers vs monolayers

How may we associate the model order-disorder transition in the phase diagrams of Figs. 4 and 9, with that of physical monolayers and bilayers?

A reasonable simplification is to take lipid-water interactions independent of the lipid state, with $\epsilon_{ow} = \epsilon_{dw} = \epsilon_{lip,w}$, for both systems. This assumption yields the following relations between monolayer and bilayer parameters [see Eqs. (8)–(11)]:

$$J^M = J^B, \tag{32}$$

$$\Delta^M = \Delta^B, \tag{33}$$

$$K^M = K^B + \left(\epsilon_{ww}^{surf} - \epsilon_{ww}^{bulk}\right) - 2\left(\epsilon_{lip,w}^{surf} - \epsilon_{lip,w}^{bulk}\right), \tag{34}$$

and

$$I^M = I^B + 4\left(\epsilon_{ww}^{surf} - \epsilon_{ww}^{bulk}\right) - 4\left(\epsilon_{lip,w}^{surf} - \epsilon_{lip,w}^{bulk}\right). \tag{35}$$

What are the implications of the difference in energy parameters for the two systems?

We first note that different K parameters imply different phase diagrams, as seen in Fig. 7(a). On the other hand, different I parameters may be adjusted to yield the same effective chemical potential μ [see Eq. (17)].

Let us first admit $K^M \approx K^B$, and analyze the equivalence hypothesis in relation to a single phase diagram, such as our pressure-temperature phase diagram of Fig. 9 or corresponding temperature-chemical potential phase diagram of Fig. 4. We consider a particular thermodynamic state for the model system, which corresponds to a point in the μ vs t phase diagram (Fig. 4), and to the same order parameter values for m and n [Eq. (24)], i.e., $m^B = m^M$ and $n^B = n^M$. It is then possible to establish a relation between the lateral pressures of the two systems in terms of our lattice model.

Lateral pressure is related to the grand potential through Eq. (30). From the definition of the grand potential [45],

$$\begin{aligned}\Phi &= \langle E\rangle - TS - \mu_{lip}N_{lip} - \mu_w N_w)\\ &= \langle E_{int} - TS - \mu N_{lip} - (\mu_w + 2\epsilon_{ww})L^2\rangle,\end{aligned} \tag{36}$$

where we have used the definitions of E_{int} and μ given by Eqs. (7) and (17), respectively.

Under the hypothesis of equal interaction parameters for both monolayers and bilayers, $K^M = K^B$, given a common thermodynamic state of same energy, entropy, and lipid density, the grand potential for the two systems will differ only through the constant terms above. Thus,

$$\Phi^B - \Phi^M = -2\left(\epsilon_{ww}^{bulk} - \epsilon_{ww}^{surf}\right)L^2. \tag{37}$$

Insertion of this result in Eq. (30), given $A = L^2 a_{ord}$, yields the following simple relation between the lateral pressures of the two systems:

$$a_{ord}\left(p_{lat}^M - p_{lat}^B\right) = 2\left(\epsilon_{ww}^{surf} - \epsilon_{ww}^{bulk}\right). \tag{38}$$

For the null pressure of the bilayer, corresponds a positive lateral pressure on the monolayer,

$$p_{lat}^M a_{ord} = 2\left(\epsilon_{ww}^{surf} - \epsilon_{ww}^{bulk}\right), \tag{39}$$

since $\epsilon_{ww}^{surf} > \epsilon_{ww}^{bulk}$.

This result gives an interpretation to the equivalence hypothesis [8–10] in terms of the statistical model. In particular, it is also in line with a phenomenological analysis proposed by Marsh [10], in which the monolayer pressure corresponding to the membrane thermodynamic state at the main transition would be numerically equal to the hydrophobic free energy density. The origin of the difference in pressures would be the

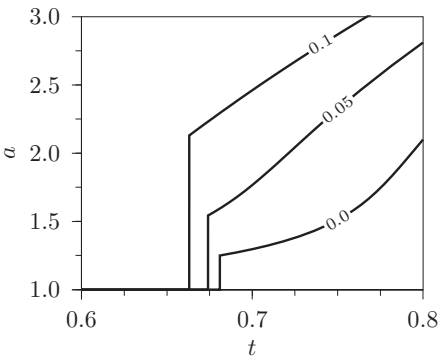

FIG. 11. Area per lipid as a function of temperature at fixed pressure for the order-disorder transition. $K/J = 1$ and $\Delta/J = 0.6$. $\Pi^{M} = 0.1$ or $\Pi^{B} = 0$ (see text) for $K^{M} = K^{B}$ and values of ϵ_{lw}/J are as indicated. Density gap decreases as mixing with water is favored.

water surface tension, a consequence of "stronger" hydrogen bonds on the surface, as compared to bulk water.

Figure 11 illustrates the behavior of the density gap for different ratios of the lipid-water interaction to water surface tension, at fixed pressure, under the artificial condition of equivalence of identical interaction constants ($K^{M} = K^{B}$). Increasing lipid-water interaction, with respect to water surface tension, transition temperature is decreased, while the area discontinuity increases.

Let us now analyze the effect of a possible difference between parameters K^{M} and K^{B}. Interactions between water molecules on the surface are more stable than between molecules in the bulk, which implies $\epsilon_{ww}^{surf} > \epsilon_{ww}^{bulk}$, while interactions between water and lipid are more favorable for the monolayer, with $\epsilon_{lip,w}^{surf} > \epsilon_{lip,w}^{bulk}$. Since water-water interactions involve larger energy values, it is to be expected that $K^{M} > K^{B}$. In this case, data for the two systems cannot be mapped onto the same phase diagram. We inspect Fig. 7(a) taking into account this point. Variation of K has two simultaneous effects. As it increases, (i) it displaces the gas-liquid line to lower chemical potential, as should be expected, since it favors lipid-lipid interactions; (ii) more importantly, it turns the order-disorder coexistence line above and near the triple point less dependent on temperature.

The latter effect has implications on the area discontinuity upon the order-disorder transition. As pointed out in the previous section, in relation to Figs. 5(b) and 5(e), the density gap diminishes as one goes away from the triple point, or, equivalently, as the Ord-Did coexistence line becomes more horizontal in the t-$\overline{\mu}$ plane (see Fig. 4). Thus, if one focuses on the transition at some specific temperature t, inspection of Fig. 7(a) shows that the discontinuity in area is smaller for larger K. This means that adopting the same transition temperature at the Ord-Dis coexistence line for systems of different interaction constant K (which may be the case for monolayers and bilayers) implies obtaining different area per lipid in the disordered phase, with a smaller area gap for the monolayer with respect to the bilayer (if $K^{M} > K^{B}$). Alternatively, if one chooses to fix the density gap, and thus a specific slope of the transition line, monolayers would yield a lower transition temperature with respect to bilayers. Interestingly, this is what happens with the experimental systems: If one looks for the equivalence at the same transition temperature, areas are different [44], with a smaller gap for monolayers. If, on the other hand, equivalence is sought from the same area gap, the two transitions are found at different temperatures, with a lower disordering temperature for monolayers.

D. Theory vs experiment

In order to discuss the adequacy of our model to describe real lipid chain transitions in vesicles and monolayers, we analyze some of our results in terms of available experimental data both on water hydrogen bond energies and on lipid layer parameters.

Precise values of hydrogen bond energies are still being investigated, and we adopt some of the recent results [46–49], in order to check our Eq. (39) which relates equivalent lateral pressure to hydrogen bond strength.

As to lipid systems, let us look at data for monolayers [50] and bilayers [44] of a specific neutral (zwitterionic) lipid, DMPC: (i) Bilayers of DMPC present the main order-disorder transition at 21 °C, with area per lipid 50 Å^2 in the ordered phase [34,51]; (ii) DMPC monolayers present order-disorder transitions between 7.5 °C and 17.5 °C, approximately [50], at lateral pressures between 10 and 37 mN/m, with minimum area per lipid 47 Å^2 in the ordered phase at the lowest temperature 7.5 °C. These data are presented in Table II. Equivalence between monolayers and bilayers has been proposed by different authors at p_{lat} ranging from 35 [10] to 50 mN/m [44].

We examine our results in the light of these data: (i) Is our Eq. (39), relating equivalent monolayer-bilayer pressure to water hydrogen-bond energies, consistent with these data? (ii) Where do we find monolayer and bilayer behavior in our phase diagrams, written in terms of dimensionless variables, particularly Fig. 10(a)?

Bilayer-monolayer equivalence. We first look at our very simple result for the monolayer lateral pressure which makes the monolayer equivalent to the tension-free bilayer, Eq .(39). This lateral pressure would depend solely on the difference between surface and bulk water bonds. We take bulk water-water bonds ϵ_{ww}^{surf} and surface water-water bonds ϵ_{ww}^{bulk} as approximately 23 and 27 kJ/mol, as suggested by the work of [46–49]. Then, for $a_{ord} = 50$ Å^2 (see Table II), Eq. (39) yields lateral pressure of $p_{lat} = 30$ mN/m, which is in very good agreement with results in the literature, which range from 30 to 50 mN/m [10,44].

Order-disorder transitions in the pressure-temperature phase diagram. Our pressure-temperature phase diagrams are

TABLE II. Monolayer vs bilayer data for DPPC.

	Ord-Dis transition temperature (°C)	Area per lipid in ordered phase (Å^2)	Lateral pressure (mN/m)
Bilayer [52]	21	50	0 (50[a])
Monolayer [50]	7.5–17.5	47–45	–

[a]Equivalent pressure for monolayers [44].

given in terms of dimensionless temperature and pressure, Eqs. (26) and (31). In Fig. 9, which represents the mean-field model phase diagram for a particular set of parameters, it can be seen that the order-disorder transition reduced temperature, $t_{\text{ord-dis}}$, ranges from 0.68 to 0.7, while the order-disorder transition pressure is above 0.1. Which region of the theoretical phase diagram may correspond to experimental points? Let us consider comparison of model and experimental data, first for bilayers, then for monolayers. (i) For the bilayer, there would be a single transition reduced temperature $t_{\text{ord-dis}}$, and a correponding single transition monolayer equivalent reduced pressure $\Pi_{\text{ord-dis}}$. For a dimensionless transition temperature $t_{\text{ord-dis}} \approx 0.7$, Eq. (26) yields a value for the interaction constant J of $\approx 6 \times 10^{-21}$ at $T = 298$ K (see Table II). In Eq. (31), together with the monolayer equivalent value for p_{lat}, and for $a_{\text{ord}} \approx 50\,\text{Å}^2$, this yields $\Pi \approx 4.2$. Thus, if data for DPPC bilayers are used, the bilayer transition point, $t^B_{\text{ord-dis}}, \Pi^B_{\text{ord-dis}}$ is at 0.7,4.2. This point is present in our model phase diagram of Fig. 9, well above the triple point. According to Figs. 4 and 5(b), the corresponding area gap is below 1%.

(ii) For the monolayer, the order-disorder transition takes place between temperatures 7.5 and 17.5. The value of J must be the same for mono- and bilayers, since it depends on lipid-lipid interactions [Eq. (8)]. Thus, for $J \approx 6 \times 10^{-21}$ J/mol, we obtain for the dimensionless temperature t the interval $t_{\text{ord-dis}} \approx 0.645$–$0.668$. Calculations for the reduced pressure of Eq. (31), based on the data of Table II, yield a range of transition pressures $\Pi_{\text{ord-dis}}$ in the approximate interval 0.75–2.9. While the pressure interval is present in the model phase diagram of Fig. 9, the temperature interval is below the triple point, and would thus be incompatible with the order-disorder transition.

The last discussion indicates that for phosphatidylcholines (PCs) we must take larger Δ values. Inspection of Fig. 10(a) shows that the area gap, in the case we have investigated most thoroughly (specific model parameters K and Δ), is too small, compared to the 20% expected for bilayers [44]. In order to make this gap nearer to the experimental values, one needs to raise the limiting temperature t_0. In the case of monolayers, one must increase the distance in temperature between the triple point and the limit for the order-disorder temperature, t_0. In both cases, this requires increasing parameter Δ, as can be seen by inspection of Figs. 4, 5(b), 5(d), and 9. This result must guide future application of the model to specific lipid dispersions.

VI. FINAL COMMENTS

We have proposed a generalization of the two-state model for lipid layers, which allows an exact description of local density. This is essential for the investigation of the effect of charges, in the case of dissociating lipids.

Inspection of model properties with respect to the relation between density and chain order led to some additional conclusions:

(i) For monolayers, the model describes both the liquid transitions (order-disorder or condensed liquid–expanded liquid), in good qualitative agreement with experimental studies.

(ii) Analysis in terms of the different model interactions between lipids and water for monolayers and bilayers yields an explanation for the difficulty in establishing the equivalence between the two experimental systems.

Further investigation of the model system in the presence of charges, both for dissociating headgroups as well as for dipolar headgroups, is under way.

ACKNOWLEDGMENTS

We thank Eduardo Henriques at Universidade Federal de Pelotas for pointing out the possibility of adapting our model to the study of monolayers and to Mario Tamashiro at Universidade Estadual de Campinas for many conversations on the theme of our work. This work is partly supported by CNPq (Conselho Nacional de Desenvolvimento Cientıifico and Tecnológico).

APPENDIX: LIMITING MODELS

Our model may be thought of as a composition of three models: (i) the original Doniach model, of density 1, (ii) a simple lattice gas, and (iii) a degenerate lattice gas. The three limiting models are obtained if one of the three values for site variables σ is discarded. Model (i) results from making site variables σ equal to 1 or -1. Model (ii) results from restricting site variables σ to 0 and $+1$. Model (iii) is obtained if site variables σ are taken as 0 or -1. Under such restrictions, each one of the three limiting models may be mapped on the two-state Ising model, given by

$$E_{\text{Ising}} = -\tilde{J} \sum_{(ij)} s_i s_j - \tilde{H} \sum_i s_i, \tag{A1}$$

where $s_i = +or - 1$. Model parameters $\tilde{J}$ and $\tilde{H}$ are different for each model, and if given in terms of our Doniach lattice solution parameters [Eqs. (8)–(10)], are as follows. For model (i),

$$\tilde{J}_{\text{i}} = J; \tag{A2}$$

$$\tilde{H}_{\text{(i)}}(T) = 4\Delta - \frac{1}{2\beta} \ln \Omega. \tag{A3}$$

For model (ii),

$$\tilde{J}_{\text{(ii)}} = \tfrac{1}{4}(J + 2\Delta + K), \tag{A4}$$

$$\tilde{H}_{\text{(ii)}}(\mu) = J + 2\Delta + K + \tfrac{1}{2}\mu. \tag{A5}$$

Finally, for model (iii), we have

$$\tilde{J}_{\text{(iii)}} = \tfrac{1}{4}(J - 2\Delta + K) \tag{A6}$$

and

$$\tilde{H}_{\text{(iii)}}(T,\mu) = J + K - 2\Delta + \frac{1}{2}\mu + \frac{1}{2\beta} \ln \Omega. \tag{A7}$$

The phase behavior of each of the three models may be obtained by adapting well-known results for the magnetic Ising

model [30]. The Ising model presents a coexistence line at $\tilde{H}^*_{\rm Ising} = 0$ which ends at a critical temperature $t_{\rm Ising}$, given by

$$t_C^{\rm Ising} \equiv \frac{k_B T_C}{\tilde{J}}. \tag{A8}$$

Thus, the critical temperature for each of the limiting models, $t_{C,x}$ [$x = $ (i),(ii),(iii)], is obtained by replacing $\tilde{J}$ with $\tilde{J}_x$ from Eqs. (A2), (A4) and (A6). The numerical value for the critical Ising temperature depends on the approach taken: Mean-field calculations overestimate it, with $t_{C,\rm MF}^{\rm Ising} = 4$, whereas the exact solution, as well as Monte Carlo simulations for large systems, yield $t_{C,\rm MC}^{\rm Ising} = 2.27$.

As a result, a coexistence line and a critical point exist for each of the three limiting models. Model (i) displays a coexistence line at fixed temperature

$$t^*_{\rm (i)} = \frac{8\overline{\Delta}}{\ln \Omega} \tag{A9}$$

between the disordered ($m = 1$) and ordered chain ($m = -1$) liquids. Model (ii) presents coexistence at fixed chemical potential

$$\mu^*_{\rm (ii)} = -2J(1 + 2\overline{\Delta} + \overline{K}), \tag{A10}$$

between a gas ($n = 0$) and a simple liquid ($n > 0$), with a critical point at

$$t_{C,\rm (ii)} = \frac{t_c^{\rm Ising}}{4}\left(1 + 2\overline{\Delta} + \overline{K}\right). \tag{A11}$$

Finally, for model (iii) a gas ($n = 0$) and a degenerate liquid ($n > 0$) coexist at

$$\mu^*_{\rm (iii)}(t) = -2J\left(1 - 2\overline{\Delta} + \overline{K} + \frac{t}{2}\ln\Omega\right), \tag{A12}$$

with a critical point at

$$t_{C,\rm (iii)} = \frac{t_c^{\rm Ising}}{4}\left(1 - 2\overline{\Delta} + \overline{K}\right). \tag{A13}$$

In the following figures we compare phase coexistence lines and critical points of our Doniach lattice solution [see Figs. 7(b) and 8] with coexistence lines for the limiting models (i)–(iii), at different values of Δ and K.

In Fig. 12 the mean-field phase diagram is shown for fixed K and different Δ. The coexistence lines of the three limiting models coincide with the coexistence lines of the DLG model away from the triple point. The critical temperature for the gas-disordered liquid line for the full model coincides with the

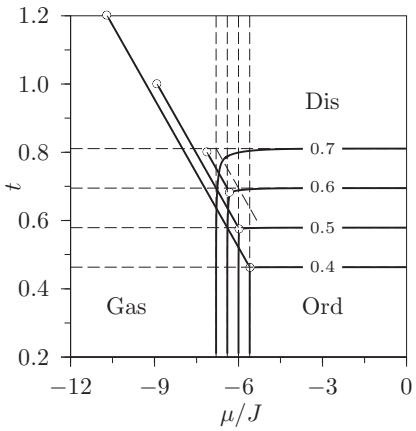

FIG. 12. Mean-field coexistence lines for DLG (continuous lines) vs coexistence lines for the limiting models (dashed lines). Doniach's model (horizontal dashed lines), lattice gas (vertical dashed lines), and degenerate lattice gas (sloped dashed lines). Critical points for the limiting models are seen only for the case of the degenerate lattice gas. For the other two limiting systems, critical points are outside the frame. For $\Delta = 0.7$, the DLG presents no Gas-Dis line. Also, the critical temperature gas-liquid line of the limiting degenerate lattice gas model is below the temperature of the Ord-Dis of the limiting Doniach model.

critical temperature of the limiting model $t_{C,\rm (iii)}$, for smaller Δ. The gas-disordered line disappears for $\overline{\Delta} = 0.7$.

In Fig. 8 points calculated from Monte Carlo simulations for the full model are displayed together with the coexistence lines and critical points of the limiting models, for $\Delta = 0.6$ and different values of K. The gas-disordered coexistence line disappears for the smaller value of K.

The crucial point is that the gas-disordered liquid coexistence line of the DLG model disappears if the critical temperature of limiting model (iii) is lower than the temperature for the chain order-disorder transition of model (i), i.e., if $t_{\rm i}^* > t_{C,\rm (iii)}$, or, from equation

$$\overline{\Delta} < \frac{(1+K)/2}{1 + \frac{16}{t_C^{\rm Ising}\ln\Omega}}. \tag{A14}$$

In the case of the mean-field results, this yields $\overline{\Delta} < 0.63$, for $\overline{K} = 1$, which explains the disappearance of the gas-disorder line for $\overline{\Delta} = 0.7$ in Fig. 12. In the case of the Monte Carlo results, this condition implies $\overline{\Delta} < 0.49$, for $\overline{K} = 1$, and $\overline{\Delta} < 0.87$, for $\overline{K} = 2.5$, which explains the presence of the Gas-Dis line only for the second case in Fig. 8.

[1] V. M. Kaganer, H. Möhwald, and P. Dutta, Rev. Mod. Phys. **71**, 779 (1999).
[2] H. Möhwald, in *Structure and Dynamics of Membranes*, edited by R. Lipowsky and E. Sackmann (North-Holland, Amsterdam, 1995), Vol. 1, Chap. 4, pp. 161–211.
[3] M. Bloom, E. Evans, and O. G. Mouritsen, Quart. Rev. Biophys. **24**, 293 (1991).
[4] S. Tristram-Nagle and J. F. Nagle, Chem. Phys. Lipids **127**, 3 (2004).
[5] J. F. Nagle, J. Chem. Phys. **58**, 252 (1973).
[6] J. F. Nagle, J. Chem. Phys. **63**, 1255 (1975).
[7] S. Marcelja, Biochim. Biophys. Acta, Biomembr. **367**, 165 (1974).
[8] J. F. Nagle, J. Membr. Biol. **27**, 233 (1976).
[9] D. W. R. Gruen and J. Wolfe, Biochim. Biophys. Acta, Biomembr. **688**, 572 (1982).
[10] D. Marsh, Biochim. Biophys. Acta, Rev. Biomembr.s **1286**, 183 (1996).

[11] M. Schneider, D. Marsh, W. Jahn, B. Kloesgen, and T. Heimburg, Proc. Natl. Acad. Sci. USA **96**, 14312 (1999).
[12] M. T. Lamy-Freund and K. A. Riske, Chem. Phys. Lipids **122**, 19 (2003).
[13] R. P. Barroso, K. A. Riske, V. B. Henriques, and M. T. Lamy, Langmuir **26**, 13805 (2010).
[14] T. A. Enoki, V. B. Henriques, and M. T. Lamy, Chem. Phys. Lipids **165**, 826 (2012).
[15] M. N. Tamashiro, C. Barbetta, R. Germano, and V. B. Henriques, Phys. Rev. E **84**, 031909 (2011).
[16] S. Doniach, J. Chem. Phys. **68**, 4912 (1978).
[17] T. R. Stouch, Mol. Simul. **10**, 335 (1993).
[18] S.-J. Marrink and H. J. C. Berendsen, J. Phys. Chem. **98**, 4155 (1994).
[19] *In Search of a New Biomembrane Model*, edited by O. G. Mouritsen and O. S. Andersen (The Royal Danish Academy of Sciences and Letters, Copenhagen, 1998).
[20] A. H. de Vries, I. Chandrasekhar, W. F. van Gunsteren, and P. H. Hünenberger, J. Phys. Chem. B **109**, 11643 (2005).
[21] A. Choutko, A. Glättli, C. Fernández, C. Hilty, K. Wüthrich, and W. van Gunsteren, Eur. Biophys. J. **40**, 39 (2011).
[22] M. J. Stevens, J. Chem. Phys. **121**, 11942 (2004).
[23] M. Venturoli, M. M. Sperotto, M. Kranenburg, and B. Smit, Phys. Rep. **437**, 1 (2006).
[24] A. E. Hac, H. M. Seeger, M. Fidorra, and T. Heimburg, Biophys. J. **88**, 317 (2005).
[25] V. Oliynyk, M. Jäger, T. Heimburg, V. Buckin, and U. Kaatze, Biophys. Chem. **134**, 168 (2008).
[26] M.-J. Huang, R. Kapral, A. S. Mikhailov, and H.-Y. Chen, J. Chem. Phys. **137**, 055101 (2012).
[27] A. Caille, A. Rapini, M. J. Zuckermann, A. Cros, and S. Doniach, Can. J. Phys. **56**, 348 (1978).
[28] O. G. Mouritsen, A. Boothroyd, R. Harris, N. Jan, T. Lookman, L. MacDonald, D. A. Pink, and M. J. Zuckermann, J. Chem. Phys. **79**, 2027 (1983).
[29] M. J. Zuckermann, D. A. Pink, M. Costas, and B. C. Sanctuary, J. Chem. Phys. **76** 4206, (1982).
[30] K. Huang, *Statistical Mechanics*, 2nd ed. (Wiley, New York, 1987).
[31] T. Heimburg, *Thermal Biophysics of Membranes (Tutorials in Biophysics)*, 1st ed. (Wiley-VCH, Weinheim, 2007).
[32] I. P. Sugár, J. Phys. Chem. B **112**, 11631 (2008).
[33] P. F. Almeida, Biophys. J. **100**, 420 (2011).
[34] V. B. Henriques, R. Germano, M. T. Lamy, and M. N. Tamashiro, Langmuir **27**, 13130 (2011).
[35] T. L. Hill, *Statistical Mechanics* (McGraw-Hill, New York, 1956).
[36] C. E. I. Carneiro, V. B. Henriques, and S. R. Salinas, Phys. A (Amsterdam, Neth.) **162**, 88 (1989).
[37] D. J. Bergman and B. I. Halperin, Phys. Rev. B **13**, 2145 (1976).
[38] J. Bruno and J. Sak, Phys. Rev. B **22**, 3302 (1980).
[39] L. K. Nielsen, T. Bjornholm, and O. G. Mouritsen, Langmuir **23**, 11684 (2007).
[40] D. Landau and K. Binder, *A Guide To Monte Carlo Simulations in Statistical Physics* (Cambridge University Press, Cambridge, 2005).
[41] K. Y. C. Lee, Ann. Rev. Phys. Chem. **59**, 771 (2008).
[42] S. Marčelja and J. Wolfe, Biochim. Biophys. Acta, Biomembr. **557**, 24 (1979).
[43] C. S. Shida and V. B. Henriques, J. Chem. Phys. **115**, 8655 (2001).
[44] J. F. Nagle and S. Tristram-Nagle, Biochim. Biophys. Acta, Rev. Biomembr. **1469**, 159 (2000).
[45] H. B. Callen, *Thermodynamics and an Introduction to Thermostatistics*, 2nd ed. (Wiley, New York, 1985).
[46] M. Smits, A. Ghosh, M. Sterrer, M. Müller, and M. Bonn, Phys. Rev. Lett. **98**, 098302 (2007).
[47] W. Gan, D. Wu, Z. Zhang, Y. Guo, and H.-F. Wang, Chin. J. Chem. Phys. **19**, 20 (2006).
[48] C. Q. Sun, X. Zhang, J. Zhou, Y. Huang, Y. Zhou, and W. Zheng, J. Phys. Chem. Lett. **4**, 2565 (2013).
[49] J. Douillard and M. Henry, J. Colloid Interface Sci. **263**, 554 (2003).
[50] D. Steppich, J. Griesbauer, T. Frommelt, W. Appelt, A. Wixforth, and M. F. Schneider, Phys. Rev. E **81**, 061123 (2010).
[51] D. Marsh, Chem. Phys. Lipids **57**, 109 (1991).
[52] G. Cevc, in *Phospholipids Handbook*, edited by G. Cevc (Marcel Dekker, New York, 1993), p. 939.